Stratoudaki, T., Clark, M., & Wilcox, P. (2015). Laser induced ultrasonic phased array using Full Matrix Capture data acquisition and Total Focusing Method. In *54th Annual British Conference of Non-Destructive Testing, NDT 2015* British Institute of Non-Destructive Testing.

Peer reviewed version

Link to publication record on the Bristol Research Portal
PDF-document

University of Bristol – Bristol Research Portal
General rights

Laser induced ultrasonic phased array using Full Matrix Capture Data Acquisition and Total Focusing Method

Theodosia Stratoudaki[1,2], Matt Clark[2] and Paul Wilcox[1]

[1] Department of Mechanical Engineering, University of Bristol, University Walk, Bristol, UK
[2] Division of Electrical Systems and Optics, Faculty of Engineering, University of Nottingham, University Park, Nottingham, UK
Telephone: +44(0)1159515556
Telefax: +44(0)1159515616
E-mail: t.stratoudaki@nottingham.ac.uk

Abstract

Laser based ultrasound is a technique where a short pulsed laser is used to generate ultrasound and optical interferometry is used in order to detect the signal. Since both generation and detection of ultrasound is based on optical means, the technique is broadband, non-contact, and couplant free, suitable for large stand-off distances, inspection of components of complex geometries and hazardous environments. A data collection method (Full Matrix Capture) developed for ultrasonic arrays, is used for data collected using laser based ultrasound. In this method, a signal is captured from every possible transmitter–receiver array element combination. After the data capture, the imaging is done in post processing using the Total Focusing Method, in which the beam is focused, in both transmission and reception, on every pixel in the image to achieve improved defect detectability and very high spatial resolution. For the first time in laser ultrasonics, the beamforming and steering of the ultrasound is done during the post processing. In this way, a synthesised 1-D laser induced ultrasonic array operates, in post processing, as a phased array without the need of complicated optical setups, optical fibres or use of multiple laser beams. This work presents results from a non destructive laser ultrasonic inspection of aluminium samples with side drilled holes and slots at depths varying between 5 and 20mm from the surface.

1. Introduction

Laser ultrasonics is a technique where lasers are used for the generation and detection of ultrasound instead of the conventional piezoelectric transducers[1,2]. The light of a pulsed laser is focused onto the surface of the component to be tested and is absorbed. In metals, the absorption of light happens at the electromagnetic skin depth, which is of the order of a few nm. Thermal diffusion further buries the source to a total of around one micron deep [3,4]. The absorbed light heats up the irradiated component causing it to expand rapidly, at times that are compared to the rise time of the laser pulse (nanoseconds duration)[5]. This fast, thermo-elastic expansion is the source of the generated ultrasonic wave. The wave then travels through the component and is detected optically, usually by some type of laser interferometer[6]. Laser ultrasonics has several advantages over conventional ultrasonic methods: it is a non contact and couplant free technique, making it suitable for places with limited access[7], hazardous

environments[8] and inspection of geometrically complex components[9]. It is also a broadband technique and all modes of ultrasonic waves (e.g. longitudinal, shear, surface waves) are excited.

The use of ultrasonic phased arrays has had a major impact on science, medicine and society, since their first appearance in the late '60s. During the last decade, there has been a rapid increase in the use of ultransonic arrays for NDT inspection. A conventional ultrasonic array is made of several ultrasonic transducer elements which can be addressed individually to transmit and receive ultrasonic signals. A phased array can control the directivity and focus of the ultrasound by varying the time delay between the firings of the array elements. The benefits of phased arrays are increased image quality and flexibility regarding the range of different inspections (e.g. plane, focused, steered) that can be done from a single location of the array. Two methods of phased arrays using laser ultrasonics have been proposed to the authors knowledge: using a single laser source with multiple optic delays and using multiple laser sources. The first method uses a single laser source which is then split and delivered to the target following a range of optical delay paths to achieve the desired time delay. This can be achieved by using multiple optical fibres of variable length[10-14], or a White cell optical delay cavity system[15]. The second method uses an array of laser cavities, fired at the desired time delay[16-18]. The disadvantage of using optical fibres for delivery of high-energy laser pulses is that the amount of energy delivered must be limited to a level that the fibre can withstand. Using a White cell optical delay cavity requires a complicated optical setup. In addition, the maximum number of elements of the phased array in both these configurations is limited by the amount of energy that a single laser source can deliver: the maximum number of phased array elements that has been achieved using a single laser source is 10 (White cell). The main disadvantage of using multiple laser sources is the cost of the system, and a second disadvantage is the portability of such a system. The maximum number of elements of a phased array achieved with a system of multiple laser sources is 16.

An alternative philosophy to array imaging is to perform the imaging in post processing. Previous authors have used the synthetic aperture focusing technique with laser ultrasonics to improve detectability and enhance images[19,20], mainly in the destructive, ablation regime. The present paper demonstrates array imaging in post processing by obtaining the full matrix of all possible transmitter receiver combinations in the array, at the non-destructive, thermoelastic regime. This data acquisition method is known as the Full Matrix Capture (FMC)[21, 22]. A major benefit of this method is that now a whole range of imaging algorithms is possible to be applied to the same data set, in post processing. For laser ultrasonics in particular, the advantage is that array configurations can now be synthesised without the need of complicated optical setups, optical fibres or use of multiple laser beams and without being limited by the physical constraints (e.g. restrictions on the number of array elements) that come with these setups.

This paper presents laser induced ultrasonic phased arrays based in the post processing of the full matrix using the total focusing method (TFM) imaging algorithm. Section 2 presents the background of the laser ultrasonic generation and detection mechanism at the non-destructive, thermoelastic regime, as well as the theory of the FMC and the TFM algoritm, adapted for laser ultrasonics. Section 3 presents the experimental setup

and experimental results from aluminium samples with side drilled holes and slots at depths ranging from 5 to 20mm from the surface. Section 4 presents a discussion of the technique, the benefits, its limitations and how to overcome them. Finally, section 5 presents the conclusions.

2. Background

2.1 Laser based ultrasound

Ultrasound is generated when the light emitted by a pulsed laser is absorbed by the material. In the low laser power thermoelastic regime there is no damage of the material and the process is non-destructive. The laser beam incident to the sample locally heats its surface and causes it to expand rapidly at times that are comparable to the rise time of the laser pulse which—for the cases considered here—is in the order of 10 ns. As the laser energy is absorbed in a layer much thinner than the ultrasonic wavelength (a few nanometres in aluminium), the bandwidth of the generated wave depends on the temporal characteristics of the laser pulse and is broadband. Longitudinal, shear and surface acoustic waves are generated. For a point source centre of expansion, the angular dependence of the amplitude of the longitudinal and the shear waves are given respectively by [5]:

$$A(\theta) = \frac{\sin\theta \sin 2\theta \ (k^2 - \sin^2\theta)^{1/2}}{2\sin\theta \sin 2\theta \ (k^2 - \sin^2\theta)^{1/2} + (k^2 - 2\sin^2\theta)^2} \quad (1)$$

$$B(\theta) = \frac{\sin\theta \cos 2\theta}{\cos^2 2\theta + 2\sin\theta \sin 2\theta \ (k^{-2} - \sin^2\theta)^{1/2}} \quad (2)$$

where θ is the observation angle with respect to the surface normal and $k = c_L/c_T$, with c_L and c_T the acoustic velocities of the longitudinal and the shear wave respectively. It has been shown[23] that the directivities of the longitudinal and shear waves for a line source are the same as those for a point source. In the case of aluminium, the directivity pattern of the longitudinal waves[17] has its maximum at $\theta = 64^\circ$ and for shear waves[23,17] the maximum is at $\theta = 30^\circ$.

2.2 Full matrix capture and total focusing method (TFM)

The full matrix capture is a data acquisition method developed for conventional ultrasonic arrays. In this method, the waveform from every possible combination of transducer/receiver of an n element array is captured and forms an n × n matrix, the full matrix. The data set can then be post processed with a range of imaging algorithms, including the Total Focusing Method (TFM). In TFM, the first step is to discretise the target region (in the x, z plane) into a grid. The signals from all elements in the array are then summed to synthesise a focus at every point in the grid[21]. The intensity of the image, I(x,z) at any point in the scan is given by [21]:

$$I(x,z) = \left| \sum_{for\ all\ tx,rx} h_{tx,rx} \left(\frac{\sqrt{(x_{tx} - x)^2 + z^2} + \sqrt{(x_{rx} - x) + z^2}}{c_{ac}} \right) \right| \quad (3)$$

$h_{tx,rx}(t)$ is the data set of the time-domain signals which ae Hilbert transforms of the experimentally obtained time-domain signals containing real and imaginary components in quadrature. x_{tx} and x_{rx} are defined in figure 2 and c_{ac} is the acoustic velocity. TFM is

an algorithm that can only be performed using FMC. It has been shown[21] that the TFM gives significantly improved resolution and signal-to-noise (SNR) compared to swept aperture plane and focused B-scans. In addition, the TFM image extends beyond the edge of the array, increasing the probability of locating defects in these locations. On the contrary, the B-scans viewable area is dependent on the number of elements used in the array. The TFM has also been shown to be a robust algorithm for a variety of defects, when compared to other widely used algorithms such as the Phase Contrast Imaging and the Spatial Compounding Imaging[24].

3. Experimental results

3.1 Experimental setup

Two aluminium samples were used in this study. The first one (sample 1, see figure 1 (a)) was a 90 x 20 x 50 mm block with four side drilled holes of 1.2mm diameter at depths 5, 8, 10 and 12mm from the surface. The second one (sample 2, see figure 1 (b)) was a 90 x 20 x 50 mm block with five side drilled slots of 1 mm length and 0.3mm width at various orientations.
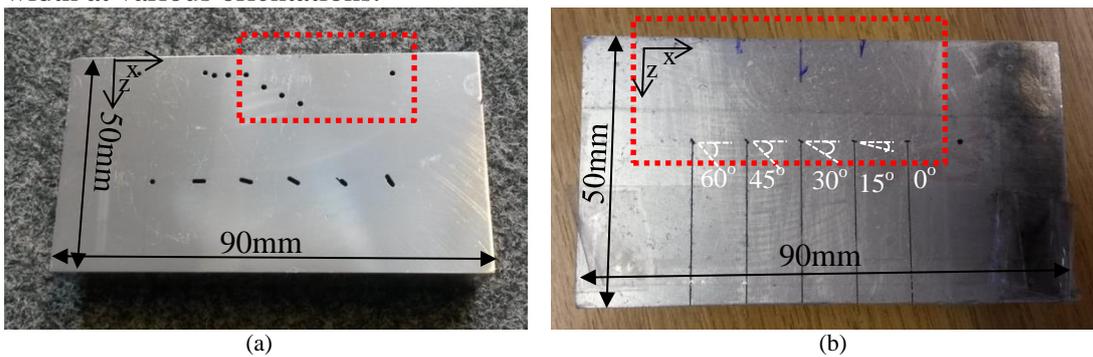
Figure 1: Photos of samples 1 (a) and sample 2 (b). Sample 1 has through holes and sample 2 has through slots of orientations ranging from 0°-60°. The red rectangle shows the holes detected in the TFM image.

The generation laser was a Nd:YAG pulsed laser with pulse rise time of 8ns and 1064nm wavelength. Its repetition rate was 1kHz and the average power 300mW, as measured in front of the sample, corresponding to 300mJ per pulse. The laser beam was focused by means of a cylindrical lens, to a line of 10mm height and 0.05mm width. The incidence angle was 25° with respect to the normal to the sample surface. Aluminium reflects 93% of the incident laser energy and only 7% is absorbed[25]. A Polytech vibrometer (OFV-534 head with OFV-5000 controller) was used to detect the ultrasonic signal, which was measuring the out-of-plane displacement. The light of the 633nm HeNe laser that it uses was focused to a 0.04mm diameter spot and was aligned with the middle of the generation line source with an angle of incidence 0° with respect to the normal. The experimental setup is depicted in figure 2.

(a)   (b)
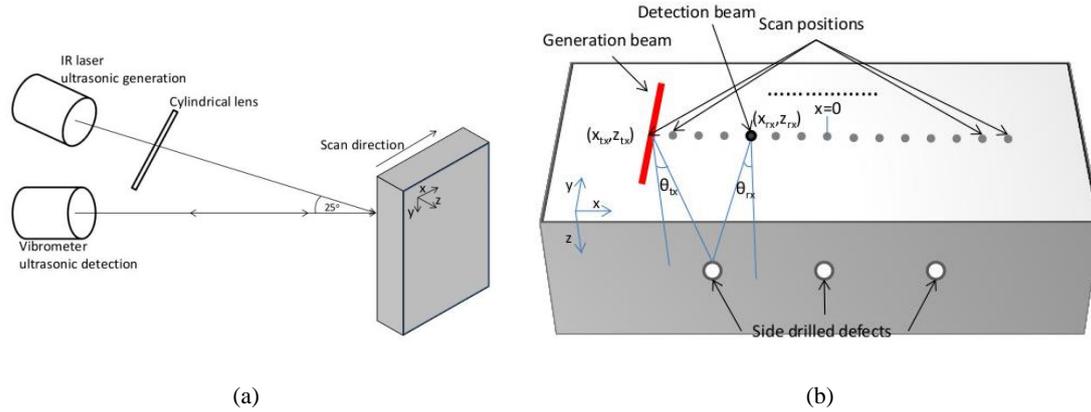
Figure 2: Experimental setup, side view (a) and top view (b). The scan was parallel to the x axis, on the xy plane, while the defects were parallel to the y-axis. (b)

During the data acquisition for the FMC, a 1-D array was synthesised. In the case of sample 1, it was a 89 element array with element spacing of 155µm and in the case of sample 2, it was a 161 element array with element spacing of 155µm. To synthesise the array in each case, the generation laser beam remained stationary throughout the experiment while the detection laser and the sample were scanned in turns. The detection laser was scanned across all consecutive element positions, while the generation laser remained focused at one position. Then the sample was moved to another element position, consequently the generation laser now irradiated another element position and the detection laser was scanned again across all element positions (figure 2). The bandwidth of the vibrometer was DC to 20MHz and there was no additional electronic filtering applied to the captured waveforms. Each captured waveform was averaged 500 times.

3.2 Results

Digital filtering was applied during the data post processing. The filters applied had central frequency of 5MHz, 8MHz or 10MHz and a 100% bandwidth, at -40dB, as specified in each case. The shear wave was chosen to image the defects as the contribution of the longitudinal wave is small in the thermoelastic regime, in metals. The shear wave velocity of 3100m/s was used in equ. (3). The directivity of the shear wave shows a max. at 30° and there was enough out-of-plane component to be detected by the vibrometer. The surface acoustic wave was present in all data and can be seen at the TFM images at the surface.

Figure 3 (a) shows the TFM image from sample 1. Four defects are very well resolved, at depths 5mm (at x=13mm from the centre of the array), 8mm (at x=-14mm from the centre of the array), 10mm (at x=-10mm from the centre of the array) and 12mm (at x=-6mm from the centre of the array). A fifth defect is just above the noise level at the far left of the image at depth 5mm (at x=17mm from the centre of the array). The B-scan composed of the same filtered data is shown in figure 3 (b). Only one defect can be seen just above the noise level. All the other defects were outside the 14mm wide aperture of the array.

Figure 4 shows the TFM image from sample 2. Five defects can be seen with high spatial resolution. Figure 5 shows a close up on the 45° angled slot of sample 2, using digital filters of 5, 8 and 10MHz central frequency. The defect can be easily identified in figure 5 (a) and (b) and it is barely above the noise level in (c). The defect is better spatially resolved in figure 5 (b) but there is a drop in the SNR by 7dB compared to figure 5 (a). The dimensions of the defect as measured from figure 5 (a) are length=2.9mm and width=0.9mm, from figure 5 (b) are length=2.3mm and width=0.6mm and from figure 5 (c) are length=2mm and width=0.4mm.

(a)

(b)
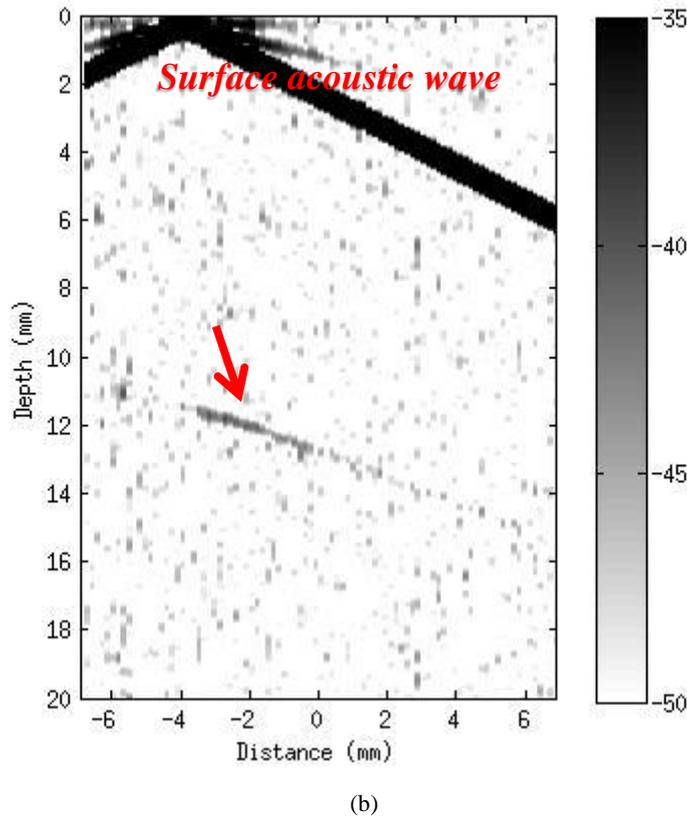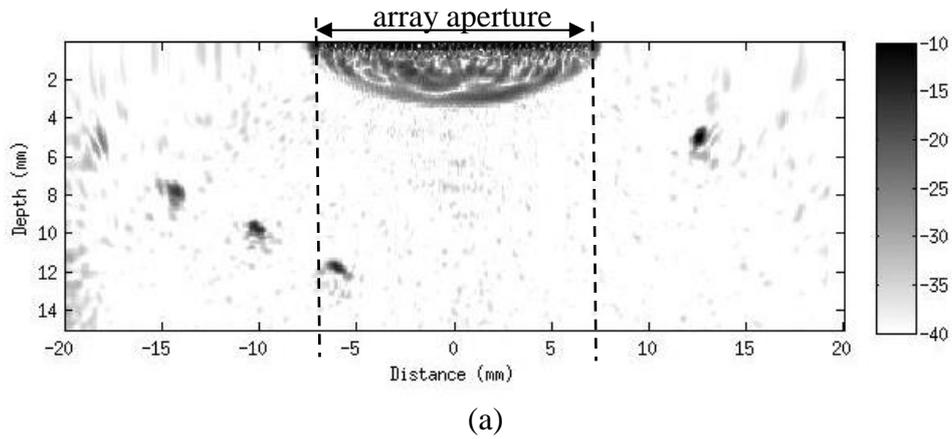
Figure 3: (a) TFM image of sample 1 using a 89 element array and 500 averages. A filter of 10MHz was applied in post processing. The dynamic range of the image is 30dB. (b) B-scan using the same data as in (a), with dynamic range of 15dB. The arrow shows the presence of the side drilled hole at 12mm.
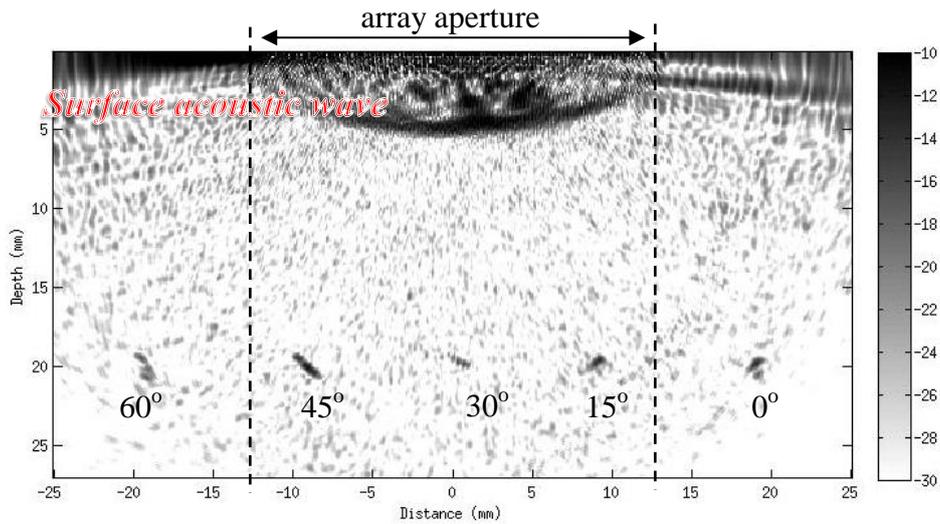
Figure 4: TFM image of sample 2 using a 161 element array and 500 averages. A filter of 8MHz was applied in post processing. The directivity of the slots is noted. The dynamic range of the image is 20dB.

        (a)   (b)   (c)
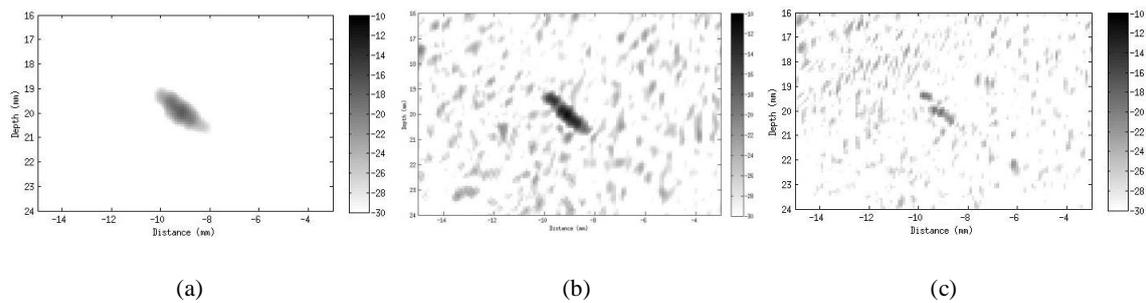
Figure 5: Detail of the TFM images showing the 45° angled slot of sample 2 using digital filter of centre frequency (a) 5MHz (b) 8MHz and (c) 10MHz. The dynamic range of all images is 20dB.

4. Discussion

Comparing figure 3 (a) and (b), there is an increase to SNR by 20dB when the TFM is used on the same data set. There is also a dramatic increase in spatial resolution of the detected defect. Another benefit of using the TFM is that defects located outside the array's aperture can be imaged, as it can be seen in all TFM images.

It is possible to perform the post process analysis in a range of frequencies, taking advantage of the broadband ultrasonic signals generated by laser ultrasonics. For the generation laser used in this study, the ultrasonic bandwidth extends from DC to 40MHz. However, the bandwidth of the detection system used (up to 20MHz) sets the upper limit. The choice of frequency for the digital filter used can be adjusted to the expected defects' size, the depth and the material properties. Figure 5 shows the post processing of the same set of data: an initial analysis at low frequencies would detect the defects and an analysis at higher frequencies would help to characterise them.

A limitation of the FMC is the need to acquire n x n signals. The procedure becomes even more time consuming when averaging of multiple signals is needed. This was the

case in the work presented here, as laser ultrasonic generation at the thermoelastic regime generally produces weak signals. Several improvements are proposed that can address this issue: (a) A laser source with higher repetition rate could be used to generate the ultrasound. A 1kHz repetition rate laser was used in this study, however a laser with repetition rate of 10kHz is just as portable and commercially available and could be used to accelerate data collection by ten times. (b) A faster oscilloscope would also improve the speed (currently using a scope with 1GHz sampling rate). (c) Lower the number of averages in the recorded signal. At a first glance, this could be achieved by increasing the generation power. However, the choice of working at the non-destructive, thermoelastic regime sets restrictions in this case. The second option is to increase the detection power and sensitivity and this can be achieved by using a different interferometer. Another option that would reduce the number of averages is to modulate the spatial intensity distribution of the generation laser beam, using Hadamard multiplexing, which has been shown to improve the SNR[26]. (d) Increase the array step and consequently the number of elements in the array. As an example, a subset of the data set collected from sample 1, was taken, corresponding to an array step of 310μm (compared to155μm of the results shown in figure 3 (a)) and a 45 element array. The resulting TFM image is shown in figure 6. Comparison of the two figures shows a drop in SNR by 5 dBs, however, the four main defects detected in figure 3, ranging in depth from 5 to 12mm, can all be easily detected. Considering the decrease in acquisition time by a factor of 2 and processing time by a factor of 30, the benefits are greater than the effect on defect detectability.
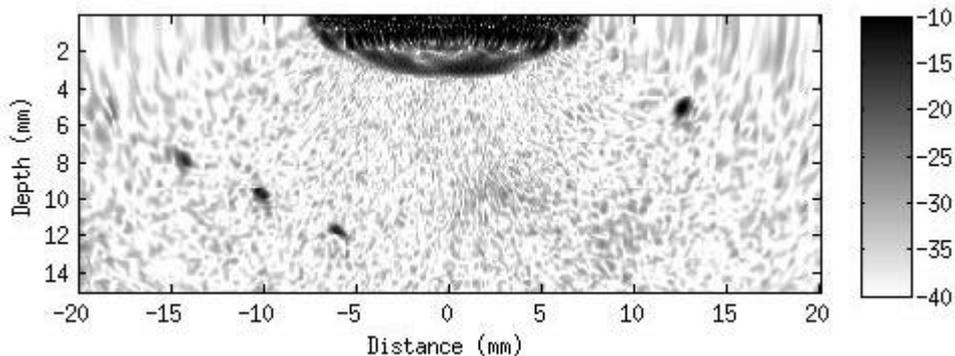
Figure 6: TFM image of subset of data for sample 1 corresponding to array step of 310μm and 45 element array. A filter of 10MHz was applied in post processing. The dynamic range of the image is 30dB.

3. Conclusions

The results presented here give the first experimental demonstration of the benefits of using the FMC data acquisition method and the TFM as a post processing algorithm in laser ultrasonics. The beamforming and steering of the ultrasound is done during the post processing resulting in a laser induced phased array with significantly improved spatial resolution and defect detectability. The technique is non-contact and non-destructive. The system can be easily fibre coupled to access difficult to reach places, and can accommodate complex geometries. The lasers themselves are relatively small and portable. The use of optics makes the array elements easy to manipulate: change spot size and scan. The FMC allows post processing in a range of different algorithms.

In this study, the same data set has been used to perform a B-scan and a TFM image. Comparison of the results has shown that the TFM allows the detection of defects outside the array aperture and improves the spatial resolution and SNR.

References and footnotes

1. S. J. Davies, C. Edwards, G. S. Taylor, and S. B. Palmer, 'Laser generated ultrasound: its properties, mechanisms and multifarious applications', J. Phys. D: Appl. Phys., Vol 26, pp 329-348, 1993.
2. C. B. Scruby and L. E. Drain, 'Laser Ultrasonics, Techniques and Applications', Bristol, UK: Adam Hilger, 1990.
3. P.A. Doyle, 'On epicentral waveforms for laser-generated ultrasound', J. Phys. D: Appl. Phys., Vol 19, pp 1613-1623, 1986.
4. K.L. Telschow and R.J. Conant 'Optical and thermal parameter effects on laser-generated ultrasound', J. Acoust. Soc. Am., Vol 88, pp 1494-1502, 1990.
5. L.R.F. Rose, 'Point-source representation for laser-generated ultrasound', J. Acoust. Soc. Am. 75(3), pp 723-732, 1984.
6. J. P. Monchalin, 'Optical detection of ultrasound', IEEE Trans. Ultrason., Ferroelectr., Freq. Control, Vol 33, No 5, pp 485–499, 1986.
7. L.-S. Wang, J.S. Steckenrider and J.D. Achenbach, 'A fiber-based laser ultrasonic system for remote inspection of limited access components', Review of Progress in Quantitative Nondestructive Evaluation, Vol 16, pp 507-514, 1997.
8. M. Dubois, M. Militzer, A. Moreau, J.F. Bussiere, 'A new technique for the quantitative real-time monitoring of austenite grain growth in steel', Scripta Materialia, Vol 42, pp 867-874, 2000.
9. K.R. Yawn, M.A. Osterkamp, D. Kaiser, C. Barina, 'Improved Laser Ultrasonic Systems for Industry', Review of Progress in Quantitative Nondestructive Evaluation, AIP Conference Proceedings, Vol 1581, pp 397-404, 2014.
10. A.J.A. Bruinsma and J.A. Vogel, 'Ultrasonic noncontact inspection system with optical fiber', Appl. Opt., Vol 27 pp 4690-4695, 1988.
11. J. Jarzynski and Y.H. Berthelot, 'The use of optical fibers to enhance the laser generation of ultrasonic waves', J. Acoust. Soc. Am., Vol 8, pp 158-162, 1989.
12. S.N. Hopko, I.C. Ume, D.S.Erdahl, 'Development of a Flexible Laser Ultrasonic Probe', J. Manufacturing Sc. and Eng., Vol 124 pp 351-357, 2002.
13. B. Mi, C. Ume, 'Real-Time Weld Penetration Depth Monitoring With Laser Ultrasonic Sensing System', J. Manufacturing Sc. and Eng., Vol 128 pp 280-286, 2006.
14. C. Pei, D. Kazuyuki, F. Tetsuo, K. Kazuyoshi, U. Mitsuru, 'Cracks measurement using fiber-phased array laser ultrasound generation', J. Appl. Phys., Vol 113, 163101, 2013.
15. J.S. Steckenrider, T.W. Murray, J.B. Deaton Jr. and J.W. Wagner, 'Sensitivity enhancement in laser ultrasonics using a versatile laser array system', J. Acoust. Sot. Am., Vol 97, pp 273-279, 1995.
16. T. W. Murray, J. B. Deaton, Jr., and J. W.Wagner, 'Experimental evaluation of enhanced generation of ultrasonic waves using an array of laser sources', Ultrasonics, Vol 34, pp 69-77, 1996.
17. M.-H. Noroy, D. Royer and M. Fink, 'The laser-generated ultrasonic phased array: Analysis and experiments', J. Acoust. Soc. Am., Vol 94, pp 1934-1943, 1993.

18. M.-H. Noroy, D. Royer and M. Fink, 'Shear-Wave Focusing with a Laser-Ultrasound Phased-Array', IEEE Trans. Ultr., Ferr. and Freq. Contrl., Vol 42, pp 981-988, 1995.
19. A. Blouin, D. Levesque, C. Neron, D. Drolet and J.-P. Monchalin, 'Improved resolution and signal-to-noise ratio in laser-ultrasonics by SAFT processing', Opt. Express, Vol 2, pp 531-539, 1998.
20. D. Levesque, A. Blouin, C. Neron, J.-P. Monchalin, 'Performance of laser-ultrasonic F-SAFT imaging', Ultrasonics, Vol 40, pp 1057–1063, 2002.
21. C. Holmes, B.W. Drinkwater, P.D. Wilcox, 'Post-processing of the full matrix of ultrasonic transmit–receive array data for non-destructive evaluation, NDT&E International, Vol 38, pp 701–711, 2005.
22. C. Holmes, B.W. Drinkwater, P.D. Wilcox, 'Advanced post-processing for scanned ultrasonic arrays: Application to defect detection and classification in non-destructive evaluation', Ultrasonics, Vol 48, pp 636–642, 2008.
23. J.R. Bernstein and J.B. Spicer, 'Line source representation for laser-generated ultrasound in aluminium', J. Acoust. Soc. Am., Vol 107, pp 1352-1357, 2000.
24. J. Zhang, B. W. Drinkwater, and P. D. Wilcox, 'Comparison of Ultrasonic Array Imaging Algorithms for Nondestructive Evaluation', IEEE Trans. Ultr., Ferr. and Freq. Contrl., Vol 60, pp 1732-1745, 2013.
25. E. D. Palik 'Handbook of Optical Constants of Solids', London: Academic, 1998.
26. G. Rousseau and A. Blouin, 'Hadamard multiplexing in laser ultrasonics', Optics Express, Vol 20, pp 25798-25816, 2012.